# Comparison of DBEM and FEM Crack Path Predictions with Experimental Findings in a notched Shaft under Torsion

**R. Citarella[1], D. Bremberg[2], F.-G. Buchholz[3]**

[1]Dept. of Mechanical Engineering, Univ. of Salerno, Fisciano (SA), Italy, rcitarella@unisa.it
[2]Department of Solid Mechanics, Royal Institute of Technology, 10044 Stockholm, Sweden
[3] retired from Institute of Applied Mechanics, University of Paderborn, Pohlweg 47-49, D-33098 Paderborn, Germany

***ABSTRACT.*** *The rather complex 3D fatigue crack growth behaviour of two anti-symmetric "bird wing" cracks, initiating from the two crack front corner points of a notched shaft undergoing torsion, is investigated by the Dual Boundary Element Method (DBEM) and by two different approaches with the Finite Element Method (FEM). In order to calculate the Stress Intensity Factors (SIFs) along the crack front four different methods are utilised: COD and J-integral in conjunction with the DBEM and the Quarter Point Element Stress method or the Modified Virtual Crack Closure Integral method in conjunction with the FEM approaches. The SIFs, calculated by such different approaches, are well consistent with each other and the simulated crack paths, based on different fracture criteria (Minimum Strain Energy Density for DBEM and* $\sigma'$ *criterion for one of the FEM approaches) qualitatively agree well among themselves and with the experimental findings.*

## INTRODUCTION

The understanding and analysis of mixed-mode fracture is an important subject in fracture mechanics because material flaws or pre-cracks can have an arbitrary orientation with respect to any service load of a component or structure. In the past, 2D crack extension problems under mixed-mode I and II loading conditions have attracted much attention and through many investigations the problem is now well understood. But for the corresponding 3D case this cannot be stated, because only a few 3D fracture criteria have been proposed so far (e.g. [1-6]) and furthermore there is a lack of experimental work on which they could be based.

In this paper some results of 3D fatigue crack growth simulations, by the Dual Boundary Element Method (using the code BEASY) and by the Finite Element Method (using the codes CURVECRACK or ADAPCRACK3D), are presented. The focus is on the different approaches for SIF's assessment and on 3D fracture criteria with related complex 3D shape or geometry of the developing crack face.

The different re-meshing strategies, adopted by DBEM and FEM in order to properly introduce one or more cracks in the base mesh, are also illustrated.

## PROBLEM DESCRIPTION

The specimen under investigation is a cylindrical shaft with a quarter-circular notch perpendicular to the shaft axis and undergoing torsion loading (Fig. 1). The geometrical shaft parameters are as follows: length L=120mm, diameter D=30mm and notch depth $a_{max}$=10mm. The material parameters used for the simulation are related to an Al-alloy and given as follows: Young's modulus E=70656 N/mm$^2$, Poisson's ratio ν=0.34, threshold-value $\Delta K_{th}$=104 N/mm$^{3/2}$ and fracture toughness $\Delta K_{IC}$=876 N/mm$^{3/2}$. The specimens are clamped at one end and subject to a cyclic axial moment equal to $M_t$=180000 Nmm on the other end. The stress ratio of the cyclic loading is R=0.1.

Fatigue crack growth originates in the experimental test specimens made of PMMA (plexiglass) and develops into two separate anti-symmetric cracks, having complex shapes, somehow similar to bird wings (Fig. 2).

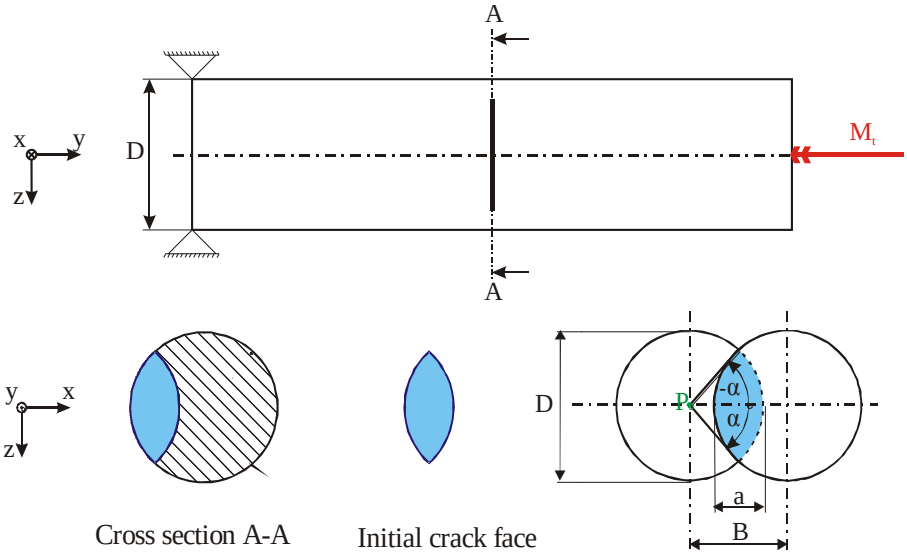


Figure 1. Cylindrical shaft under torsion, with a quarter-circular notch.

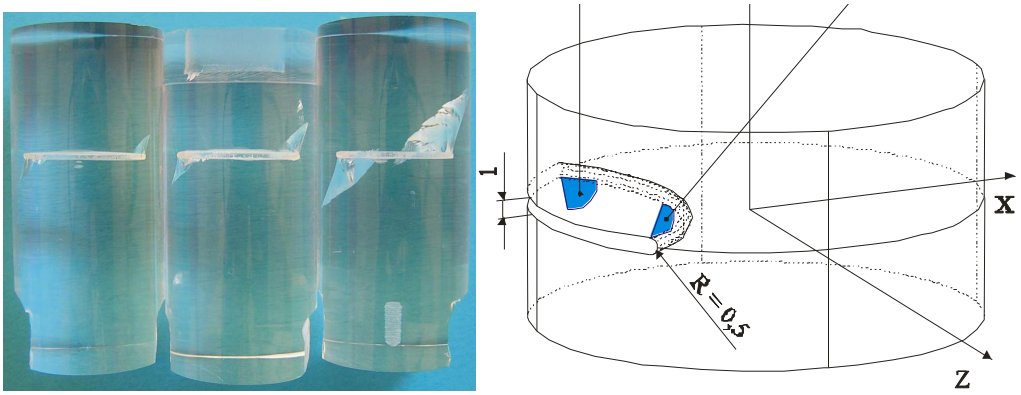


Figure 2. Experimentally obtained cracks in the PMMA shaft with a quarter-circular notch under torsion (left) and sketch of initially modeled cracks (right).

## DBEM and FEM NUMERICAL ANALYSIS

### *DBEM analysis*

In the DBEM approach, two distinct and discontinuous initial cracks, have to be incorporated into the shaft model realized by the BEASY code [7]. Their spatial orientation, defined and denoted by a kink angle $\varphi_0$=+-69° and a twist angle $\psi_0$=-13° (Fig. 3), is based on the information provided by the preliminary investigation on the overall quarter circular crack (the notch was modeled as a quarter circular crack and one step of propagation realized to assess the initial crack propagation angles at $\alpha/\alpha_{max}$=+-1 as provided in Fig. 3 [8-9]). In Fig. 4 the DBEM shaft model is shown in the initial configuration and after one increment with $a_{max}$=0.7 mm along the crack front, with highlight of the maximum principal stresses (a different deformation scale is adopted for the two configurations). The convergent initial model is based on 3316 triangular and quadrilateral elements with quadratic interpolation for both geometry and functional variables (the total number of degrees of freedom is 63204). The elements on the crack are discontinuous. SIF's are calculated by both J-integral and Crack Opening Displacement (COD) methods: the former resorts to a numerical integration on the J-path based on 4 segments, 4 arcs and 5 internal points per arc; whereas the latter uses the COD calculated on the middle node of each crack front element.

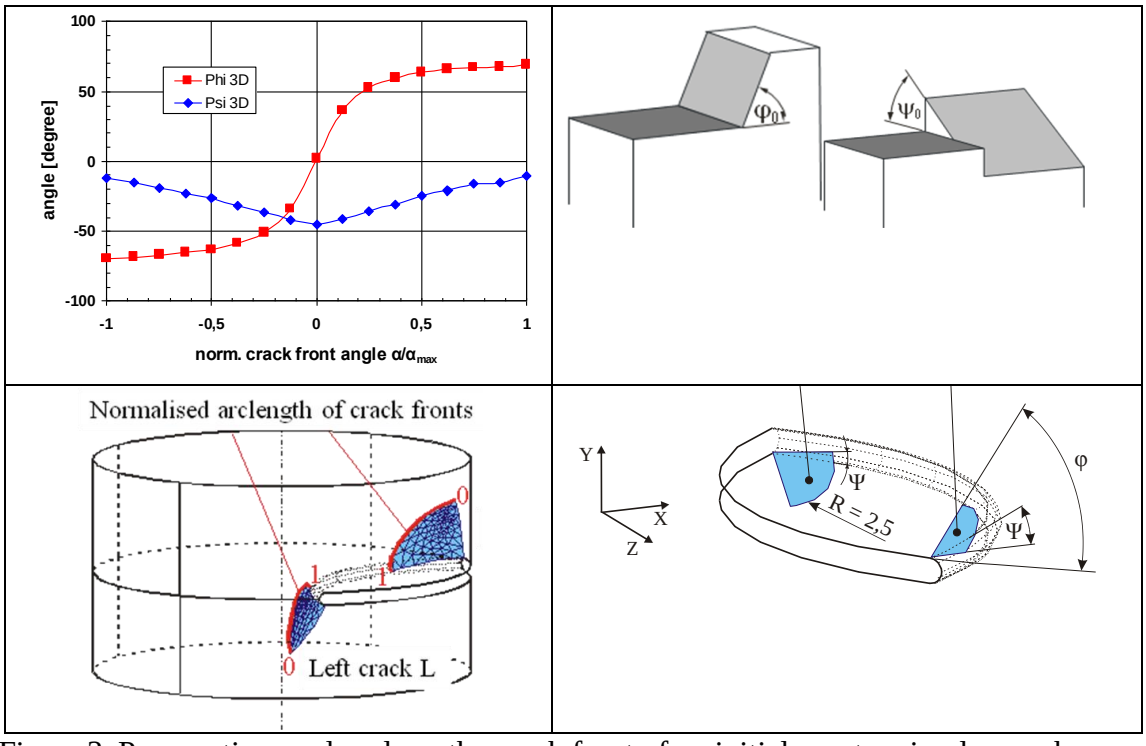


Figure 3. Propagation angles along the crack front of an initial quarter circular crack modeling the notch (left): mode II kink angle φ and mode III twist angle ψ (right).

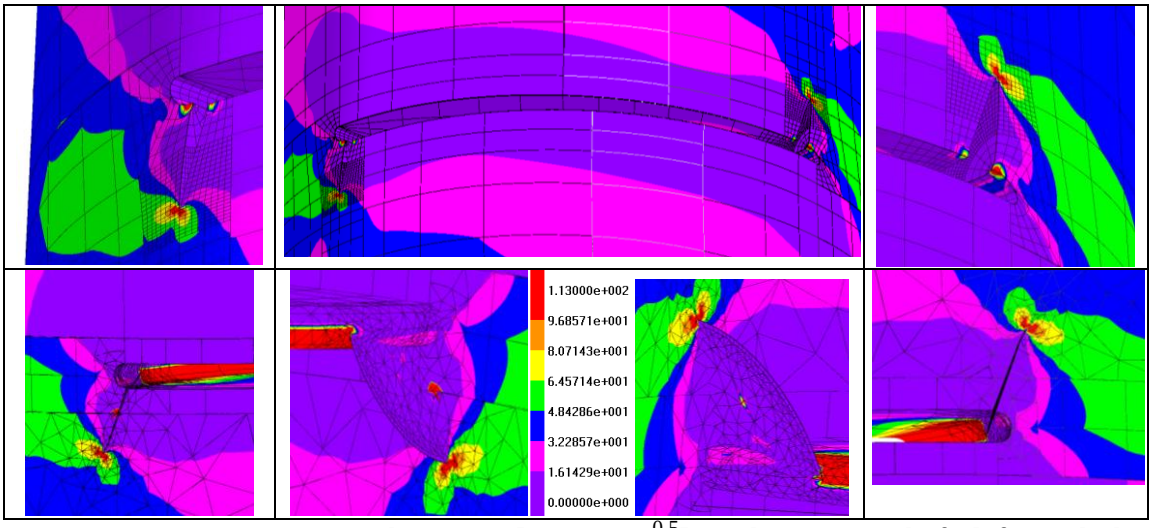

Figure 4. Maximum principal stresses [MPa*mm$^{0.5}$] on the DBEM shaft deformed plot with close up of the initial cracks (up) and of the grown cracks (after one step).

***FEM Analysis by the code CURVEDCRACK on the initial crack configuration***

Crack growth computations require the existing input mesh to be manipulated and/or adapted to the prevailing crack front and crack surface configuration. The strategy used in CURVEDCRACK is to govern the preprocessing by the shape and location of the crack front. A selection of elements from the initial input mesh is replaced by a new mesh including the crack front and crack faces. The preprocessing consists of four steps:

1. A tubular domain is set up along the crack front enclosing its neighbourhood. It is filled with a focused and well structured hexahedral mesh, similar to a spider's web, with collapsed quarter point elements in direct connection with the crack front.
2. A transition domain can be identified as the difference between the domain set up by the selection of elements from the initial mesh and the tubular hexahedral mesh. This transition domain is filled with tetrahedral elements.
3. The three separate meshes are connected by linear constraint equations usually referred to as multiple point constraint (MPC) equations.
4. Initial conditions and loads such as temperature and residual quantities are interpolated from the selected elements of the initial mesh to the new mesh since the nodes and integration points of the two meshes are not coincident.

The structured tubular mesh does not only yield singular fields matching the analytical singular expressions for the SIFs but also simplifies and enhances bookkeeping capabilities for postprocessing activities. Another important advantage of the method is the independence of the type of input mesh. Since a selection of elements are replaced and connected by MPCs, the input mesh does not have to be supplied in a specific type. The major benefit, however, is the capability of modelling curved crack fronts and non-planar crack surfaces without restrictions imposed by built-in constraints. Once the stress field has been established by use of any generic FE-software, post-processing may commence. To compute the SIFs, the singular FE-stress field is compared directly to the

asymptotic analytical expressions. In order to avoid the decision whether plane stress or plane strain prevails, only the stress components acting in the local crack front plane are considered. It gives rise to three unknowns ($K_I$,$K_{II}$ and $K_{III}$) which are obtained by a least squares computation including the five analytical equations by the Quarter Point Element Stress method (indicated as "QP" in Fig. 7). Figure 5 shows a magnification of the left crack region illustrating the three separate meshes that together constitute the cracked mesh. The pre- and post-processing are described in [10] and a comparison with another crack propagation software CRACKTRACER and reference handbook solutions is presented in [11]. The shaft input mesh is given by quadratic hexahedral elements.

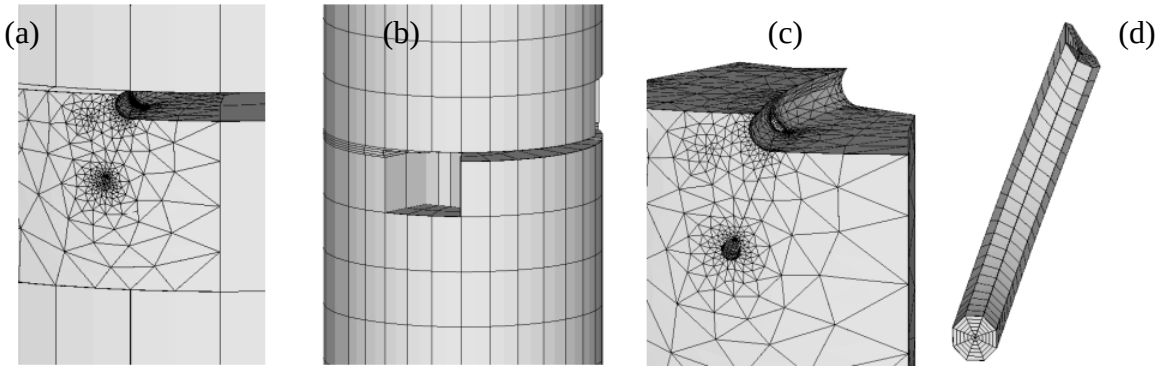


Figure 5. The cracked mesh (a) consists of intact initial input mesh with selected elements removed (b), the transition tetrahedral mesh (c) and the tubular hexahedral mesh (d).

***FEM analysis by the code ADAPCRACK3D***

Experimental crack scenarios at different stages of crack propagation and the corresponding FEM simulations by ADAPCRACK 3D are illustrated in Fig. 6.

In ADAPCRACK3D the numerically accurate and robust Modified Virtual Crack Closure method (MVCCI) [9] is utilized in order to calculate the Strain Energy Release Rates (SERRs) along the crack front, based on nodal point forces and nodal point displacements (local energy method). The SERRs are transferred into SIF's using Irwins well known formulae under the assumption of plane strain along the two crack fronts. The incremental crack propagation assessment is based on the $\sigma$' criterion [5].

## DBEM AND FEM RESULTS

At first the fracture analysis results presented in Fig. 7a will be discussed. It is the finding that for both initial cracks (left and right) KI is highly predominant and KII and KIII are found to be several magnitudes smaller. This confirms that the approximation of the "initial bird wing cracks" through small cracks with a circular crack front, plane crack faces and the orientation taken from the pre-analysis (angles $\varphi_o$ and $\psi_o$) is admissible and furthermore provides reasonably good results (if the generalized principle of local symmetry is adopted, KII and KIII should be found to be zero along

the crack fronts). In particular the ADAPCRACK3D results, which are based on a rather coarse mesh, could be improved through a refined crack front meshing. But here this could not be achieved automatically, due to the complex intersection geometry between the cracks and the notch. More pronounced this difference can be seen in the KII and KIII diagrams of Fig. 7b due to the other scaling. In Fig. 8, FEM (by ADAPCRACK3D) and DBEM SIFs along the crack front are shown, after a first increment with a maximum crack advance of respectively $a_{maxFEM}$=1 mm and $a_{maxDBEM}$=0.7 mm.

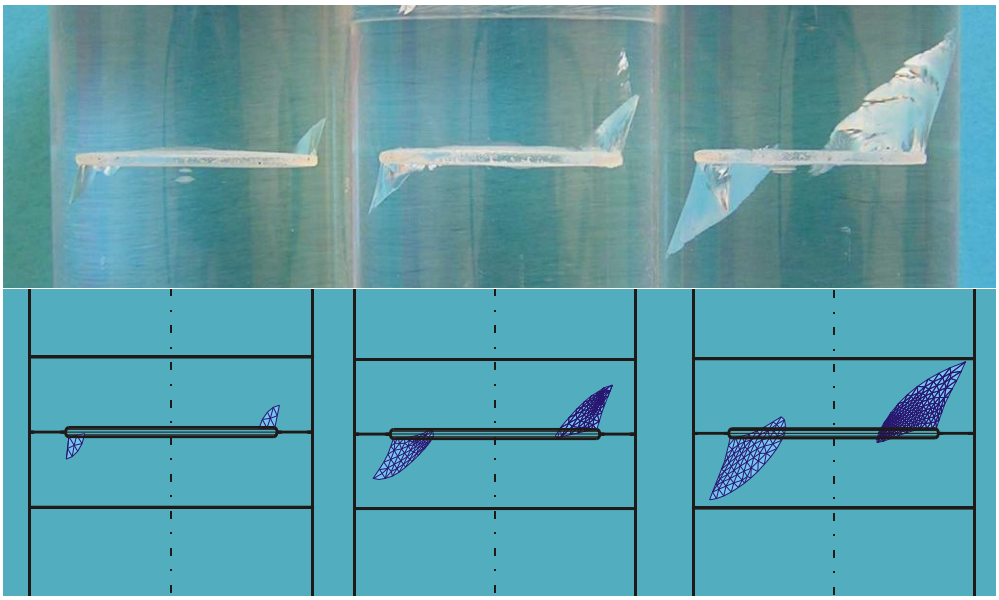

Figure 6. Comparison of experimentally obtained and simulated cracks.

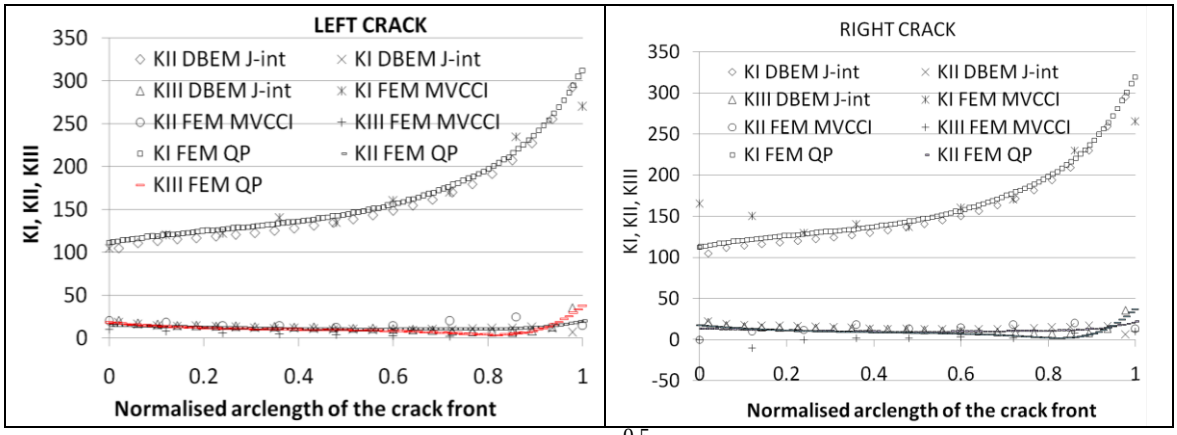


Fig. 7a. DBEM and FEM SIF's [MPa*mm$^{0.5}$] along the two initial crack fronts.

## CONCLUSIONS

In this paper some results of computational 3D fatigue crack growth simulations have been presented. The computational results are found to be in good agreement between

DBEM and FEM approaches, both in the initial configuration and after one step of crack propagation (even if, in the latter case the maximum crack advances adopted in FEM and DBEM simulations were slightly different). Consequently, also for this case of a SEN-specimen under torsion loading the functionality of the three codes (BEASY, CURVEDCRACK and ADAPCRACK3D) and the validity of the proposed 3D fracture criteria is confirmed.

Moreover it can be pointed out the higher efficiency of the DBEM approach in the pre-processing phase, due to the inherent method peculiarities (lower mesh dimensionality).

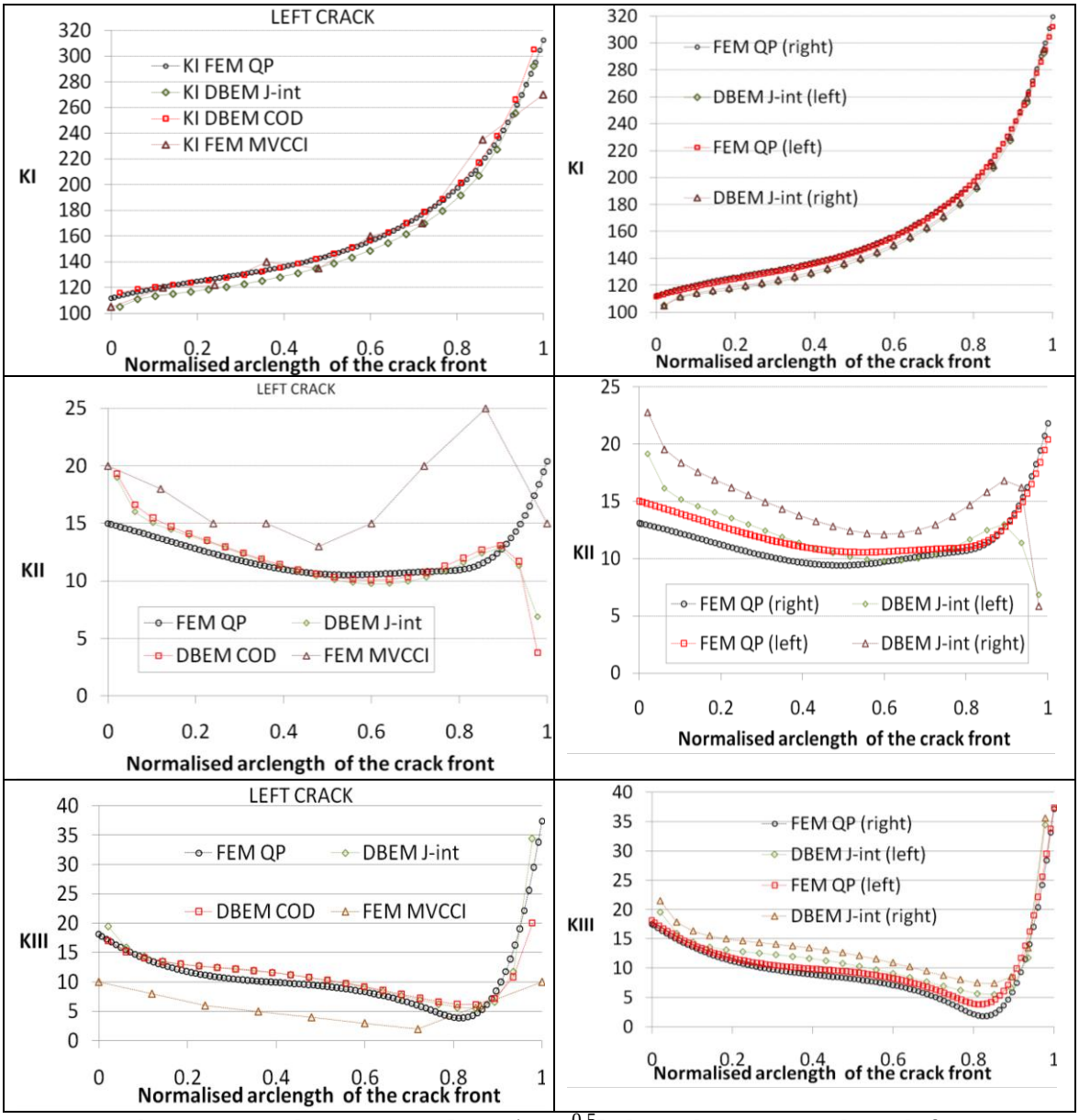


Fig. 7b. DBEM and FEM SIF's [MPa*mm$^{0.5}$] along the two initial crack fronts.

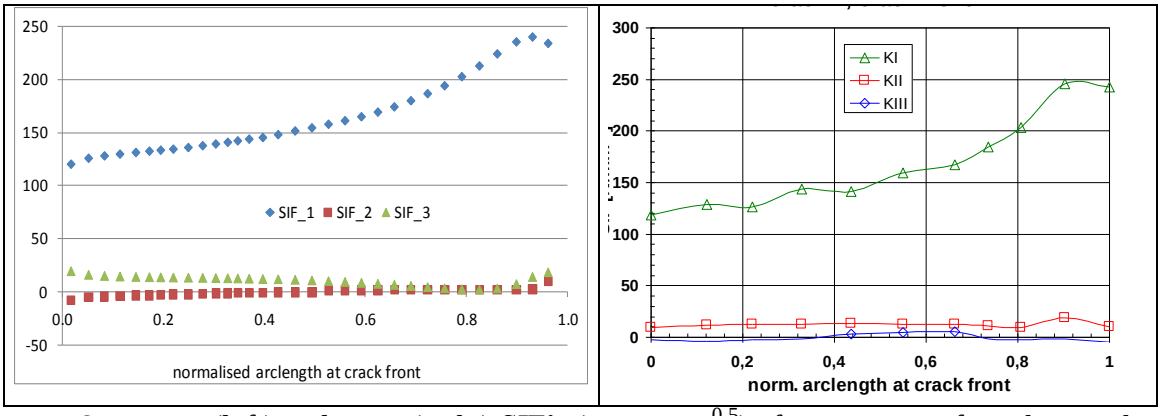


Fig. 8. DBEM (left) and FEM (right) SIF's (MPa*mm$^{0.5}$) after one step of crack growth (the FEM and DBEM maximum crack advances differ by 0.3 mm).

## REFERENCES


[1] M.K. Kassir, G.C. Sih, "Three dimensional crack problems", *Mechanics of Fracture*, 2, Noordhoff, Leyden, 1975.

[2] L.P. Pook, "On fatigue crack paths", *Int. J. Fatigue*, 17, 5-13, 1995.

[3] V. Lazarus, J.-B. Leblond, "Crack paths under mixed mode I+II or (I+II+III) loadings" *Comptes Rendus de l´Academie des Sciences, Serie* ***II***, 326 (3), 171-177, 1998.

[4] G. Dhondt, "A New Three-Dimensional Fracture Criterion", *Key Engineering Materials*, Vol. 251-252 (2003), pp. 209-214.

[5] M. Schöllmann, H.A. Richard, G. Kullmer, M. Fulland, "A new criterion for the prediction of crack development in multiaxially loaded structures", *Int. J. Fract.* 117, 129-141, 2002.

[6] G.C. Sih, B.C.K. Cha, "A fracture criterion for three-dimensional crack problems", *Journal of Engineering Fracture Mechanics* 6, 699-732, 1974.

[7] BEASY, BEASY V10r10 Documentation, C.M. BEASY Ltd, (2009).

[8] R. Citarella, M. Lepore, F.-G. Buchholz, J. Wiebesiek, Comparison of DBEM crack path predictions with experimental findings and FE results in a shaft under torsion. In: Atti del XXXVII Convegno Nazionale AIAS. XXXVII Convegno Nazionale AIAS, Roma. 10-13 settembre 2008. (vol. cd, pp. 1-10). ISBN/ISSN: 978-88-87965-51-3. ANCONA: clua edizioni (ITALY).

[9] F.-G. Buchholz, J. Wiebesiek, M. Fulland and H. A. Richard, "Comparison of Computational Crack Path Predictions with Experimental Findings for a Quarter-Circular Surface Crack in a Shaft under Torsion", Key Engineering Materials, Vol. 348-349 (2007) pp. 161-164.

[10] Bremberg D, Dhondt G (2008) Automatic crack-insertion for arbitrary crack growth. Eng Frac Mech 75:404-416.

[11] Bremberg D, Dhondt G (2009) Automatic 3-D crack propagation calculations: a pure hexahedral element approach versus a combined element approach. Int J Fract DOI: 10.1007/s10704-009-9313-z.